J|A|C|S
ARTICLES
Published on Web 10/02/2004

Synthesis and Properties of Monodisperse Oligofluorene-Functionalized Truxenes: Highly Fluorescent Star-Shaped Architectures

Alexander L. Kanibolotsky,[†,‡] Rory Berridge,[†] Peter J. Skabara,*[,†] Igor F. Perepichka,*[,§] Donal D. C. Bradley,[⊥] and Mattijs Koeberg[⊥]

Contribution from the Department of Chemistry, University of Manchester, Manchester M13 9PL, U.K., L. M. Litvinenko Institute of Physical Organic and Coal Chemistry, National Academy of Sciences of Ukraine, Donetsk 83114, Ukraine, and Blackett Laboratory, Imperial College London, London SW7 2BZ, U.K.

Received October 24, 2003; E-mail: peter.skabara@man.ac.uk; i_perepichka@yahoo.com

Abstract: This paper describes the strategy toward novel monodisperse, well-defined, star-shaped oligofluorenes with a central truxene core and from monofluorene to quaterfluorene arms. Introduction of solubilizing *n*-hexyl groups at both fluorene and truxene moieties results in highly soluble, intrinsically two-dimensional nanosized macromolecules **T1**−**T4**. The radius for the largest oligomer of ca. 3.9 nm represents one of the largest known star-shaped conjugated systems. Cyclic voltammetry experiments reveal reversible or quasi-reversible oxidation and reduction processes (E_{ox} = +0.74 to 0.80 V, E_{red} = −2.66 to 2.80 eV vs Fc/Fc^+), demonstrating excellent electrochemical stability toward both p- and n-doping, while the band gaps of the oligomers are quite high (E_g^{CV} = 3.20−3.40 eV). Close band gaps of 3.05−3.29 eV have been estimated from the electron absorption spectra. These star-shaped macromolecules demonstrate good thermal stability (up to 400−420 °C) and improved glass transition temperatures with an increase in length of the oligofluorene arms (from T_g = 63 °C for **T1** to 116 °C for **T4**) and show very efficient blue photoluminescence (λ_{PL} = 398−422 nm) in both solution (Φ_{PL} = 70−86%) and solid state (Φ_{PL} = 43−60%). Spectroelectrochemical experiments reveal that compounds **T1**−**T4** are stable electrochromic systems which change their color reversibly from colorless in the neutral state (∼340−400 nm) to colored (from red to purple color; ∼500−600 nm) in the oxidized state.

Introduction

Star polymers, which are usually defined as branched macromolecules that consist of linear polymer arms joined together by a central core, have been of great interest in the past decade.[1] A star-shaped architecture combined with conjugated character within the arms would bring new electrical, optical, and morphological properties to the system which, depending on the structure of the central core, could have intrinsic two- or three-dimensional character. Monodisperse, well-defined π-conjugated oligomers have recently become one of the most promising prospects in materials science, allowing a deep insight into the photophysics of conjugated systems and the interpretation of the supramolecular structure of conjugated polymers.[2] In this context, star-shaped conjugated architectures have attracted increasing attention as possible alternatives to linear conjugated oligomers in optoelectronic applications (light-emitting devices (LED), photovoltaics, field-effect transistors, etc.).[3]

Over the past decade, polyfluorenes have emerged as leading electroluminescent materials with bright blue emission, high hole mobility, and easily tunable properties through modifications and copolymerizations.[4] Recently, Lin et al. reported on starlike polyfluorenes with a silsesquioxane core.[5] Many linear oligofluorenes have been synthesized and studied as model compounds of polyfluorenes.[6] In contrast to conjugated polymers, monodisperse oligomers are characterized by a well-defined and uniform molecular structure as well as superior chemical purity, which can be easily reached, for example, by column chromatography. These intrinsic features allow a deep insight into the effects of chemical structure on electronic, photonic, and

[†] University of Manchester.
[§] National Academy of Sciences of Ukraine.
[⊥] Imperial College London.
[‡] On leave from the National Academy of Sciences of Ukraine.

(1) Hadjichristidis, N.; Pitsikalis, M.; Pispas, S.; Iatrou, H. *Chem. Rev.* **2001**, *101*, 3747−3792.
(2) *Electronic Materials: The Oligomeric Approach*; Müllen, K., Wegner, G., Eds.; Wiley-VCH: Weinheim, New York, 1998.
(3) (a) Li, B.; Li, J.; Fu, Y.; Bo, Z. *J. Am. Chem. Soc.* **2004**, *126*, 3430−3431. (b) de Bettignies, R.; Nicolas, Y.; Blanchard, P.; Levillain, E.; Nunzi, J.-M.; Roncali, J. *Adv. Mater.* **2003**, *15*, 1939−1943. (c) Ponomarenko, S. A.; Kirchmeyer, S.; Elschner, A.; Huisman, B.-H.; Karbach, A.; Drechsler D. *Adv. Funct. Mater.* **2003**, *13*, 591−596. (d) Cherioux, F.; Guyard, L. *Adv. Funct. Mater.* **2001**, *11*, 305−309.
(4) (a) Grice, A. W.; Bradley, D. D. C.; Bernius, M. T.; Inbasekaran, M.; Wu, W. W.; Woo, E. P. *Appl. Phys. Lett.* **1998**, *73*, 629−631. (b) Redecker, M.; Bradley, D. D. C.; Inbasekaran, M.; Wu, W. W.; Woo, E. P. *Adv. Mater.* **1999**, *11*, 241−246. (c) Bernius, M. T.; Inbasekaran, M.; O'Brien, J.; Wu, W. *Adv. Mater.* **2000**, *12*, 1737−1750. (d) Scherf, U.; List, E. J. W. *Adv. Mater.* **2002**, *7*, 477−487. (e) Leclerc, M. *J. Polym. Sci. A, Polym. Chem.* **2001**, *39*, 2867−2873. (f) Whitehead, K. S.; Grell, M.; Bradley, D. D. C.; Jandke, M.; Strohriegl, P. *Appl. Phys. Lett.* **2000**, *76*, 2946−2948.
(5) Lin, W.-J.; Chen, W.-C.; Wu, W.-C.; Niu, Y.-H.; Jen, A. K.-Y. *Chem. Mater.* **2004**, *37*, 2335−2341.

morphological properties of materials. From a practical standpoint, chemical purity and uniformity are often critical parameters of the performance of LEDs. Several publications demonstrated that the performance and the stability of monodisperse oligofluorenes in LEDs are higher than those for polyfluorenes,[6d] in which fast degradation and an appearance of undesirable green emission during the LED operation are observed due to formation of fluorenone defects on the polymer chain.[7] In the absence of chain entanglements or defects (e.g., bends or kinks), relatively short conjugated chains are believed to be conducive to the formation of monodomain films. However, oligomers are generally more inclined to form a crystalline state than polymers, which can scatter the light and limit charge injection and transport in LEDs. In this regard, oligomeric materials capable of demonstrating a glass transition state while resisting crystallization are better candidates for LED applications.

10,15-Dihydro-5*H*-diindeno[1,2-*a*;1′,2′-*c*]fluorene (truxene, **1**), a polycyclic aromatic system with C_3 symmetry,[8] has been recognized as a potential starting material for the construction of bowl-shaped fragments of the fullerenes,[9] C_3 tripodal materials in chiral recognition,[10] and liquid crystalline compounds.[11,12] Some *syn*-trialkylated truxenes (monoalkylated at each CH_2 group) have been shown to self-associate in solution through arene−arene interactions.[13] Recently, Echavarren and co-workers synthesized a series of sterically crowded 5,10,15-triarylated truxenes (aryl = 1- or 2-naphthyl, 9-phenanthryl, 9-anthracenyl). They also prepared overcrowded 5,10,15-tri(9-fluorenylidene)truxene, which showed reversible reduction peaks in cyclic voltammetry at −0.94, −1.18, and −1.45 V (vs SCE).[14] Truxene can be considered as three "overlapping" fluorene fragments, and in this sense it represents an excellent choice as a core for construction of two-dimensional star-shaped oligofluorenes. Its CH_2 groups can be easily functionalized (e.g., by alkyl subsituents to increase the solubility and processability of the materials) in the same manner as that exploited in oligo/polyfluorenes; subsequent oligomers constituting oligofluorene arms and the central truxene core can be virtually considered as "no-core" star-shaped oligofluorenes. Recently, Pei and co-workers reported on employing the truxene core for star-shaped oligothiophene architectures and an elegant synthesis of truxene-based dendrimers.[15]

Chart 1

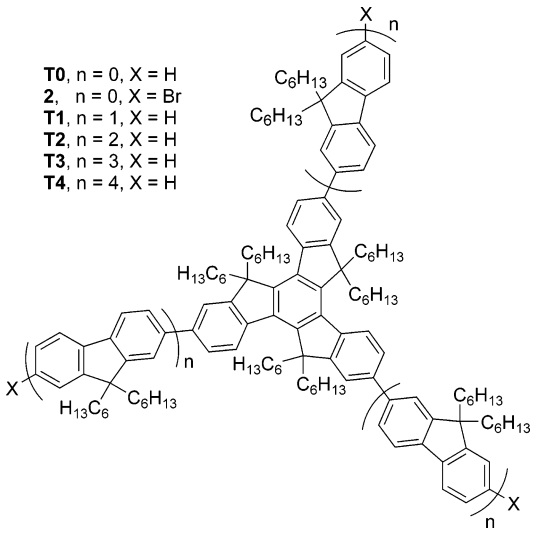

In this paper, we describe the strategy toward novel monodisperse, star-shaped oligofluorenes **T1**−**T4** (Chart 1) with a central truxene core and up to quaterfluorene arms, which results in nanosized macromolecules. In the case of **T4**, the radius of the macromolecule is ca. 4 nm, which represents the largest known star-shaped conjugated system. We also report on their highly efficient blue light emission, together with high thermal and electrochemical stability.

Results and Discussion

Synthesis. The strategy used in the synthesis of truxene-oligofluorenes **T1**−**T4** was different from the repetitive divergent approach exploited by Pei and co-workers for the design of star-shaped oligomers (an increase of the arm size by repetitive addition of arm units to the star-shaped oligomer through Suzuki coupling).[15a,16] In our case, the divergent method gave very low yields, and the separation of the desired oligomers from mono- and disubstituted byproducts and homocoupling

(6) (a) Geng, Y.; Trajkovska, A.; Culligan, S. W.; Ou, J. J.; Chen, H. M. P.; Katsis, D.; Chen, S. H. *J. Am. Chem. Soc.* **2003**, *125*, 14032−14038. (b) Geng, Y.; Trajkovska, A.; Katsis, D.; Ou, J. J.; Culligan, S. W.; Chen, S. H. *J. Am. Chem. Soc.* **2002**, *124*, 8337−8347. (c) Wong, K.-T.; Chien, Y.-Y.; Chen, R.-T.; Wang, C.-F.; Lin, Y.-T.; Chiang, H.-H.; Hsieh, P.-Y.; Wu, C.-C.; Chou, C. H.; Su, Y. O.; Lee, G.-H.; Peng, S.-M. *J. Am. Chem. Soc.* **2002**, *124*, 11576−11577. (d) Geng, Y.; Culligan, S. W.; Trajkowska, A.; Wallace, J. U.; Chen, S. H. *Chem. Mater.* **2003**, *15*, 542−549. (e) Geng, Y.; Chen, A. C. A.; Ou, J. J.; Chen, S. H. *Chem. Mater.* **2003**, *15*, 4352−4360. (f) Culligan, S. W.; Geng, Y.; Chen, S. H.; Klubek, K.; Vaeth, K. M.; Tang, C. W. *Adv. Mater.* **2003**, *15*, 1176−1180. (g) Lee, S. H. Nakamura, T.; Tsutsui, T. *Org. Lett.* **2001**, *3*, 2005−2007. (h) Klaerner, G.; Miller, R. D. *Macromolecules* **1998**, *31*, 2007−2009.

(7) (a) List, E. J. W.; Guentner, R.; de Freitas, P. S.; Scherf, U. *Adv. Mater.* **2002**, *14*, 374−378. (b) Gaal, M.; List, E. J. W.; Scherf, U. *Macromolecules* **2003**, *36*, 4236−4237. (c) Gong, X.; Iyer, P. K.; Moses, D.; Bazan, G. C.; Heeger, A. J.; Xiao, S. S. *Adv. Funct. Mater.* **2003**, 13, 325−329.

(8) Gómez-Lor, B.; de Frutos, Ó.; Ceballos, P. A.; Granier, T.; Echavarren, A. M. *Eur. J. Org. Chem.* **2001**, 2107−2114.

(9) (a) Abdourazak, A. H.; Marcinow, Z.; Sygula, A.; Sygula, R.; Rabideau, P. W. *J. Am. Chem. Soc.* **1995**, *117*, 6410−6411. (b) Demlow, E. V.; Kelle, T. *Synth. Commun.* **1997**, *27*, 2021−2031. (c) Plater, M. J.; Praveen, M.; Howie, A. R. *J. Chem. Res. (S)* **1997**, 46−47; *J. Chem. Res. (M)* **1997**, 0430−0436. (d) Gómez-Lor, B.; de Frutos, Ó.; Echavarren, A. M. *Chem. Commun.* **1999**, 2431−2432. (e) Gómez-Lor, B.; González-Cantalapiedra, E.; Ruiz, M.; de Frutos, Ó.; Cárdenas, D. J.; Santos, A.; Echavarren, A. M. *Chem. Eur. J.* **2004**, *10*, 2601−2608.

(10) For the review on C_3-symmetrical receptors, see: Moberg, C. *Angew. Chem., Int Ed.* **1998**, *37*, 248−268.

(11) (a) Destrade, C.; Malthete, J.; Tinh, N. H.; Gasparoux, H. *Phys. Lett. A* **1980**, *78*, 82−84. (b) Tinh, N. H.; Malthete, J.; Destrade, C. *Mol. Cryst. Liq. Cryst.* **1981**, *64*, 291−298. (c) Destrade, C.; Gasparoux, H.; Babeau, A.; Tinh, N. H.; Malthete, *J. Mol. Cryst. Liq. Cryst.* **1981**, *67*, 693−703. (d) Foucher, P.; Destrade, C.; Tinh, N. H.; Malthete, J.; Levelut, A. M. *Mol. Cryst. Liq. Cryst.* **1984**, *108*, 219−230. (e) Tinh, N. H.; Foucher, P.; Destrade, C.; Levelut, A. M.; Malthete, J. *Mol. Cryst. Liq. Cryst.* **1984**, *111*, 277−292. (f) Raghunathan, V. A.; Madhusudana, N. V.; Chandrasekhar, S.; Destrade, C. *Mol. Cryst. Liq. Cryst.* **1987**, *148*, 77−84. (g) Buisine, J. M.; Cayuela, R.; Destrade, C.; Tinh, N. H. *Mol. Cryst. Liq. Cryst.* **1987**, *144*, 137−160.

(12) (a) Perova, T. S.; Vij, J. K. *Adv. Mater.* **1995**, *7*, 919−922. (b) Sandstroem, D.; Nygren, M.; Zimmermann, H.; Maliniak, A. *J. Phys. Chem.* **1995**, *99*, 6661−6669. (c) Fontes, E.; Heiney, P. A.; Ohba, M.; Haseltine, J. N.; Smith, A. B. *Phys. Rev. A* **1988**, *37*, 1329−1334. (d) Lee, W. K.; Wintner, B. A.; Fontes, E.; Heiney, P. A.; Ohba, M.; Haseltine, J. N.; Smith, A. B. *Liq. Cryst.* **1989**, *4*, 87−102. (e) Lee, W. K.; Heiney, P. A.; Ohba, M.; Haseltine, J. N.; Smith, A. B. *Liq. Cryst.* **1990**, *8*, 839−850. (f) Maliszewskyj, N. C.; Heiney, P. A.; Blasie, J. K.; McCauley, J. P.; Smith, A. B. *J. Phys. II* **1992**, *2*, 75−85. (g) Goldfarb, D.; Belsky, I.; Luz, Z.; Zimmermann, H. *J. Chem. Phys.* **1983**, *79*, 6203−6210.

(13) (a) de Frutos, Ó.; Gómez-Lor, B.; Granier, T.; Monge, M. Á.; Gutiérrez-Puebla, E.; Echavarren, A. M. *Angew. Chem., Int. Ed.* **1999**, *38*, 204−207. (b) (a) de Frutos, Ó.; Granier, T.; Gómez-Lor, B.; Jiménez-Berbero, J.; Monge, Á.; Gutiérrez-Puebla, E.; Echavarren, A. M. *Chem. Eur. J.* **2002**, *8*, 2879−2890.

(14) Ruiz, M.; Gómez-Lor, B.; Santos, A.; Echavarren, A. M. *Eur. J. Org. Chem.* **2004**, 858−866.

(15) (a) Pei, J.; Wang, J.-L.; Cao, X.-Y.; Zhou, X.-H.; Zhang, W.-B. *J. Am. Chem. Soc.* **2003**, *125*, 9944−9945. (b) Cao, X.-Y.; Zhang, W.-B.; Wang, J.-L.; Zhou, X.-H.; Lu, H.; Pei, J. *J. Am. Chem. Soc.* **2003**, *125*, 12430−12431.

(16) Zhou, X.-H.; Yan, J.-C.; Pei, J. *Org. Lett.* **2003**, *5*, 3543−3546.

Scheme 1. Synthesis of Hexahexyltruxene (**T0**) and Tribromo-hexahexyltruxene **2**

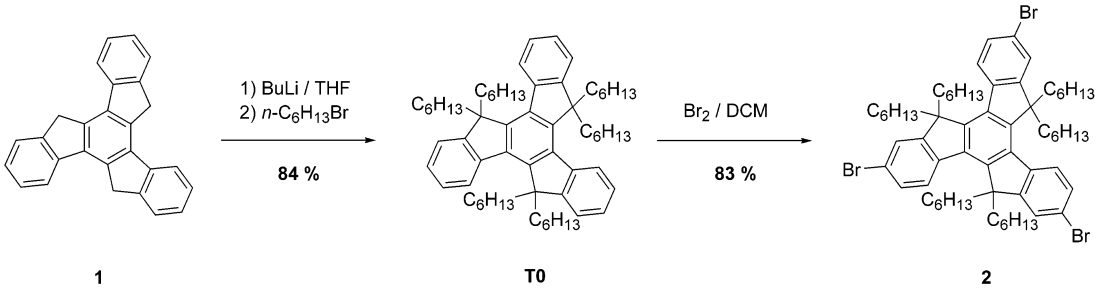

Scheme 2. Synthesis of Oligofluorene-2-boronic Acids **F1**, **F2**, **F3**, and **F4**, and 2-Bromo-oligofluorenes **5**, **6**, and **7**

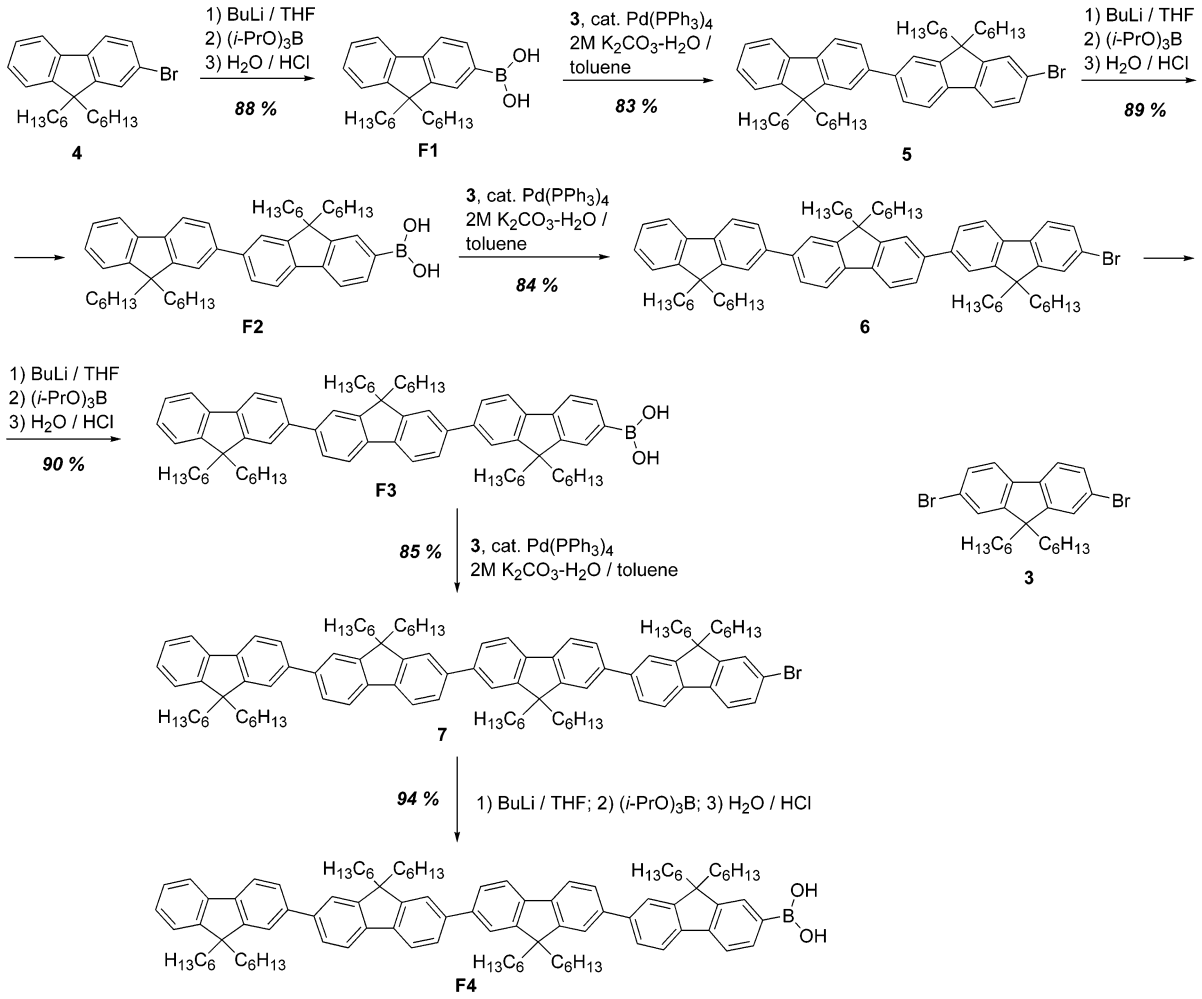

byproducts proved difficult. Instead, we attached oligofluorene arms of corresponding length directly to the central truxene core of **T0**. For this purpose we first synthesized, starting from truxene **1**, the hexahexylated truxene core with bromine terminal substituents **2** (Scheme 1), exploiting procedures similar to those described for alkylation[17] and bromination[18] of fluorene in the synthesis of 2,7-dibromo-9,9-dihexylfluorene **3**.

The synthesis of 2-bromo-oligofluorenes **5**−**7** and oligofluorene-2-boronic acids **F1**−**F4** is depicted in Scheme 2. In general, we used a repetitive procedure for the conversion of bromo derivatives **4**−**7** into the corresponding boronic acids **F1**−**F4** via lithiathion with *n*-BuLi, followed by quenching with triisopropyl borate and hydrolysis under acidic conditions. The boronic acids were then coupled by Suzuki methodology with 2,7-dibromo-9,9-dihexylfluorene **3**, affording the next generation of 2-bromo-oligofluorene (a 3-fold excess of **3** over boronic acids **F1**−**F3** was used to diminish bis-coupling at both sides of 2,7-dibromo 9,9-dihexylfluorene **3**).

It is known that arylboronic acids form dimers through intermolecular hydrogen bonding[19] or infinite networks in the case of polyfunctional boronic acids.[20] As a result, OH protons are often "invisible" in their ^{1}H NMR spectra. Moreover, they easily lose water, yielding the corresponding tricyclic anhydrides, boroxines.[21] In our case, we observed this when comparing the ^{1}H NMR spectra of "as obtained" fluorene boronic acids (from the column after purification) with the spectra of

(17) (a) Ranger, M.; Leclerc, M. *Chem. Commun.* **1997**, 1597−1598. (b) Ranger, M.; Rondeau, D.; Leclerc, M. *Macromolecules* **1997**, *30*, 7686−7691.
(18) Cho, H. N.; Kim, J. K.; Kim, D. Y.; Kim, C. Y.; Song, N. W.; Kim, D. *Macromolecules* **1999**, *32*, 1476−1481.

Scheme 3. Dehydration of Fluorene Boronic Acids **F1**−**F4** into Boroxines **F1b**−**F4b**

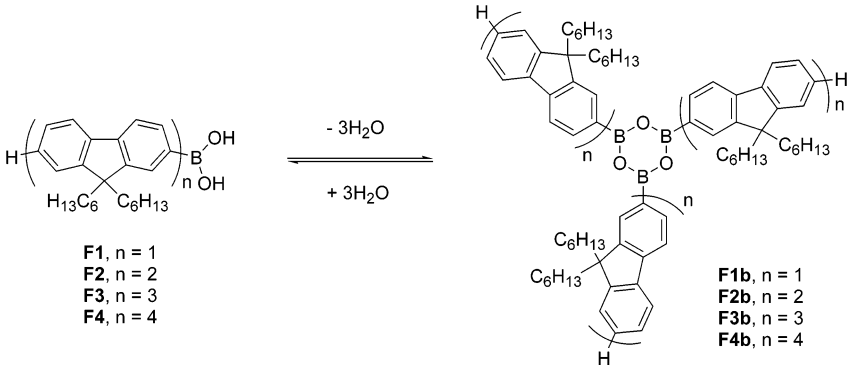

Table 1. Fluoreneboronic Acids **F1**, **F2**, **F3**, and **F4**

	calculated (acid), %				calculated (anhydride), %				found, %		
compd	M_W, g mol^{-1}	C	H	B	M_W, g mol^{-1}	C	H	B	C	H	B
F1	378.36	79.36	9.32	2.86	1081.02	83.33	9.23	3.00	82.79	9.39	2.81
F2	710.88	84.48	9.50	1.52	2078.58	86.67	9.46	1.56	86.32	9.82	1.49
F3	1043.40	86.33	9.56	1.04	3076.15	87.85	9.53	1.05	87.30	9.63	1.16
F4	1375.92	87.29	9.60	0.79	4073.71	88.45	9.58	0.80	87.49	9.84	0.87

Scheme 4. Suzuki-Coupling Route to **T1** and **T2** Truxene-Fluorene Oligomers

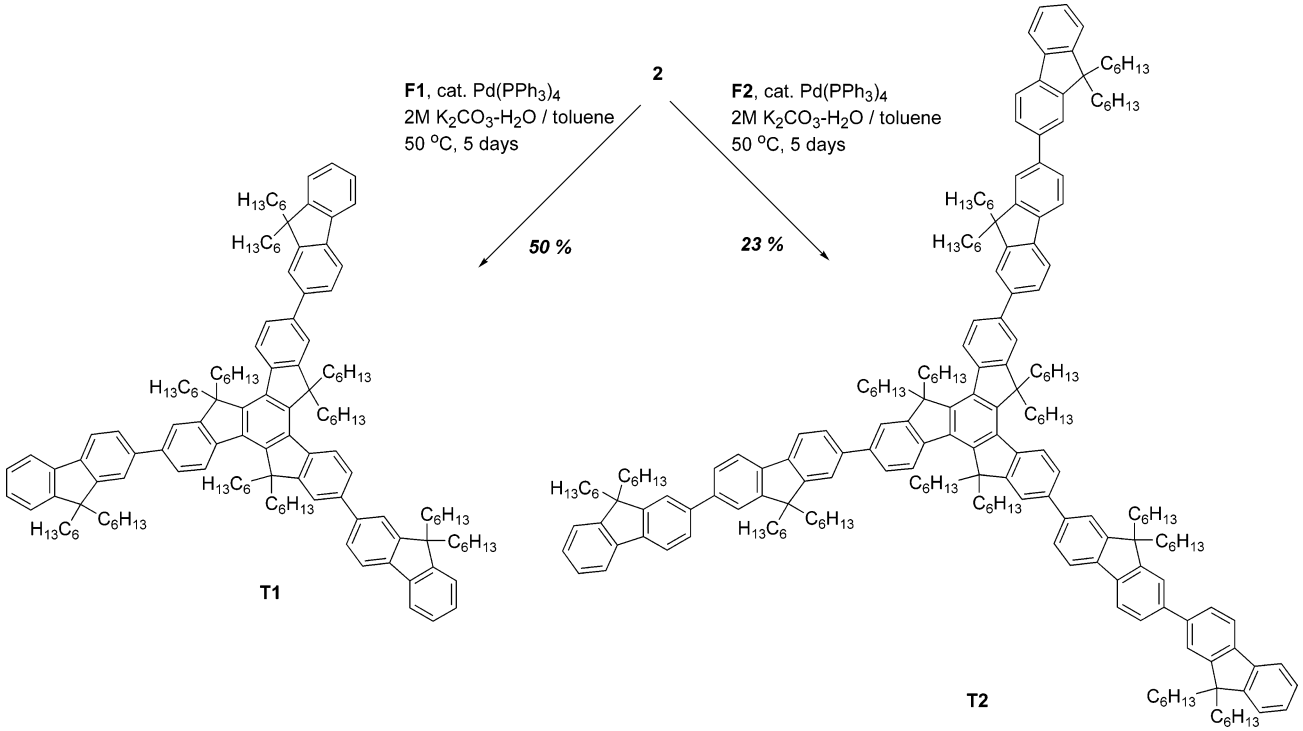

the same samples when they were dried in vacuo at 40−70 °C. Initially complicated spectra became simpler as a result of the transformation of the acids into boroxines (Scheme 3). According to elemental analyses (the analysis on carbon is the most sensitive for this transformation), drying the samples converted fluorene-2-boronic acids **F1** and **F2** almost completely into the corresponding boroxines (Table 1), whereas the longer fluorene chain products probably existed as a mixture of the acid and the boroxine.

Because the reactivities of both boronic acids and boroxines are similar and the presence of water in the Suzuki coupling reaction results in the hydrolysis of boroxines back to the acids, we use the term "fluorene boronic acids" throughout the paper,

(19) (a) Rettig, S. J.; Trotter, J. *Can. J. Chem*. **1977**, *55*, 3071−3075. (b) Zhdankin, V. V.; Persichini, P. J., III; Zhang, L.; Fix, S.; Kiprof, P. *Tetrahedron Lett*. **1999**, *40*, 6705−6708. (c) Schilling, B.; Kaiser, V.; Kaufmann, D. E. *Chem. Ber*. **1997**, *130*, 923−932. (d) Akita, T.; Kobayashi, K. *Adv. Mater*. **1997**, *9*, 346−348. (e) Bradley, D. C.; Harding, I. S.; Keefe, A. D.; Motevalli, M.; Zheng, D. H. *J. Chem. Soc., Dalton Trans*. **1996**, 3931−3936. (f) Pilkington, M.; Wallis, J. D.; Larsen, S. *J. Chem. Soc., Chem. Commun*. **1995**, 1499−1500. (g) Gainsford, G. J.; Meinhold, R. H.; Woolhouse, A. D. *Acta Crystallogr., Sect. C* **1995**, *C51*, 2694−2696. (h) Scouten, W. H.; Liu, X.-C.; Khangin, N.; Mullica, D. F.; Sappenfield, E. L. *J. Chem. Cryst*. **1994**, *24*, 621−626. (i) Soundararajan, S.; Duesler, E. N.; Hageman, J. H. *Acta Crystallogr., Sect. C* **1993**, *C49*, 690−693. (j) Feulner, H.; Linti, G.; Noth, H. *Chem. Ber*. **1990**, *123*, 1841−1843.

(20) Fournier, J.-H.; Maris, T.; Wuest, J. D.; Guo, W.; Galoppini, E. *J. Am. Chem. Soc*. **2003**, *125*, 1002−1006.

(21) (a) Li, W.; Nelson, D. P.; Jensen, M. S.; Hoerrner, R. S.; Cai, D.; Larsen, R. D.; Reider, P. J. *J. Org. Chem*. **2002**, *67*, 5394−5397. (b) Wu, Q. G.; Wu, G.; Brancaleon, L.; Wang, S. *Organometallics* **1999**, *18*, 2553−2556.

Scheme 5. Negishi-Coupling Route to **T2**, **T3**, and **T4** Truxene-Fluorene Oligomers

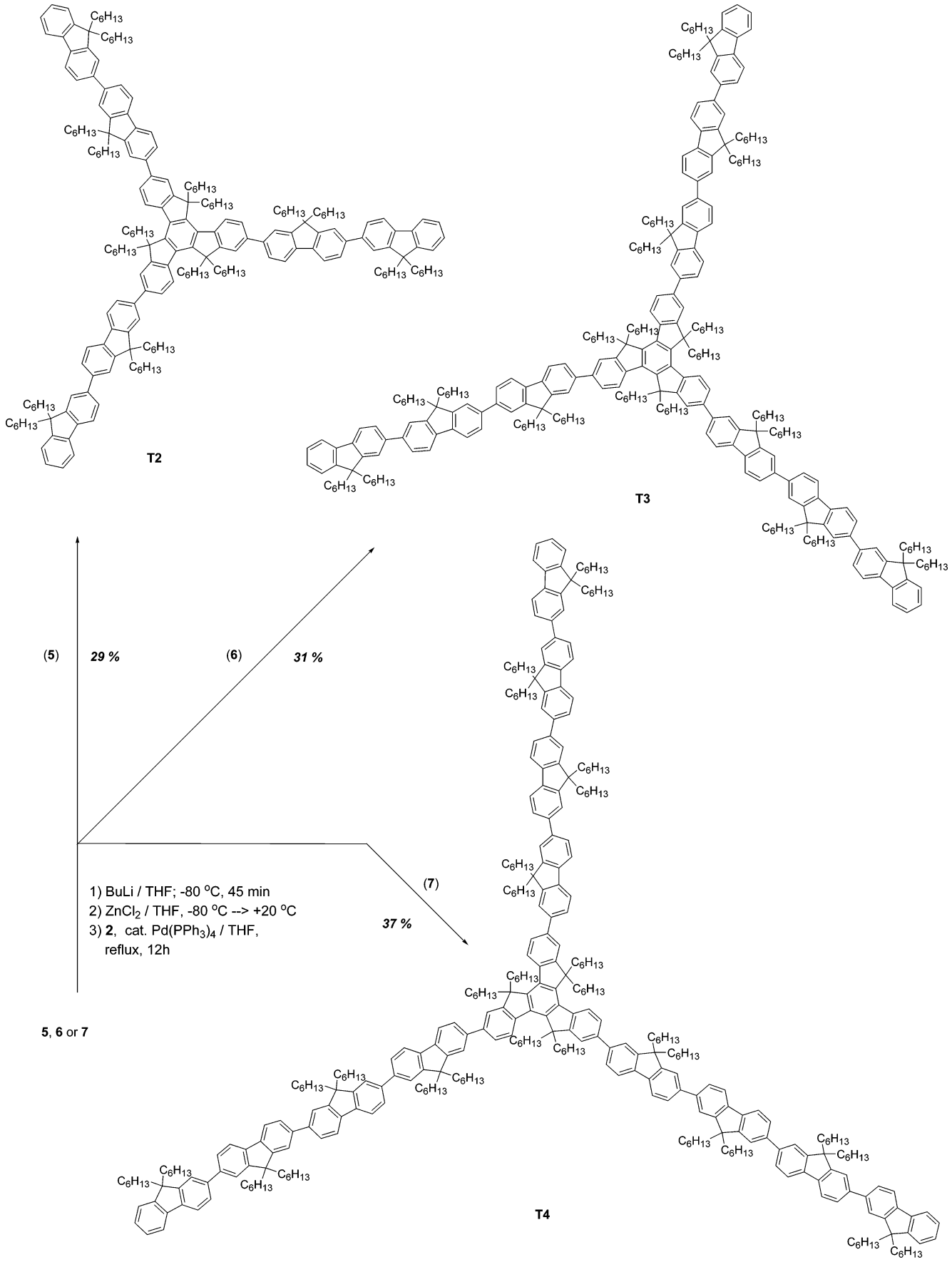

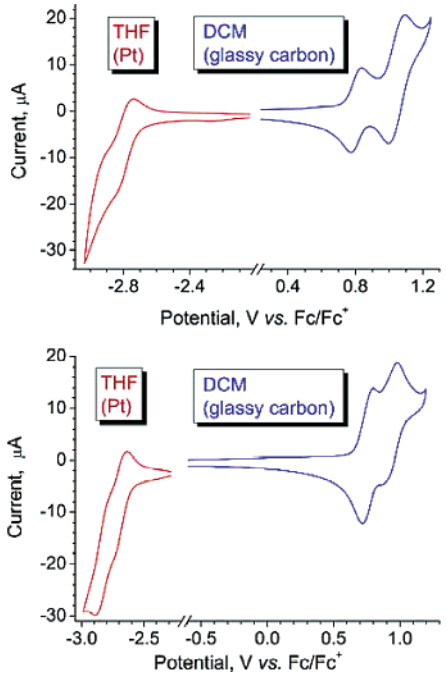

Figure 1. Cyclic voltammogram of truxene-fluorene derivatives **T1** (top) and **T3** (bottom); electrolyte 0.1 M Bu_4NPF_6, scan rate 100 mV s^{-1}.

Table 2. CV Data for Compounds **T1**−**T4**

compd	$E_{ox}^{1/2}$,[a] V vs Fc/Fc+	$E_{red}^{1/2}$,[b] V vs Fc/Fc+	E_g^{CV},[c] eV
T1	0.80, 1.05	−2.80	3.40
T2	0.76, 0.84, 1.03	−2.74	3.30
T3	0.76, 0.94	−2.70, −2.83	3.24
T4	0.74, 0.87	−2.66, −2.74	3.20

[a] DCM, 0.1 M Bu_4NPF_6, 100 mV s^{-1}. [b] THF, 0.1 M Bu_4NPF_6, 100 mV s^{-1}. [c] Band gap estimated from the onsets for the reduction and oxidation peaks.

understanding, however, that the isolated compounds were (after drying) the boroxines in some cases.

For shorter oligomers **T1** (yield 50%) and **T2** (yield 23%), we used Suzuki cross-coupling of 2-fluorene(bifluorene) boronic acids with tribromotruxene derivative **2** (Scheme 4). For the synthesis of longer oligomers, we prepared 9,9-dihexylated 2-bromo-oligofluorenes by an iterative procedure of Suzuki coupling of (*n*)-fluorene-2-boronic acids with an excess of 9,9-dihexyl-2,7-dibromofluorene (**3**), resulting in (*n*+1)-fluoren-2-yl bromides (in these syntheses the yields achieved were good to excellent, 83−94%); see also ref 22. The monobromo-oligomers were then converted into zinc derivatives via reaction with BuLi and $ZnCl_2$ for Negishi type cross-coupling with **2**, affording derivatives **T2**−**T4** in 29−37% yields (Scheme 5). Oligomers **T1**−**T4** were adequately characterized by ^1H and ^{13}C NMR, MALDI-TOF MS, and elemental analyses data.

Electrochemistry. Cyclic voltammetry (CV) experiments were conducted to probe the electrochemical properties of the oligomers. The results revealed two sequential single-electron reversible oxidation peaks [in dichloromethane (DCM)] and reversible or partly reversible reductions [in tetrahydrofuran (THF)], demonstrating good electrochemical stability of the oligomers toward both p- and n-doping (Figure 1, Table 2).

Whereas the reduction of the oligomers **T1**−**T4** to radical anions demonstrated regular positive shifts from −2.80 to −2.66 V (vs Fc/Fc^+), the oxidation processes were more complex (although a negative shift in the first oxidation peaks from +0.80 to +0.74 V in the range of **T1**−**T4** was observed). For longer oligomers **T3** and **T4**, current values for the first and second oxidation waves are very close, indicating that the same number of electrons are involved in both oxidation processes. Due to partial overlapping of the first and second oxidation waves, the difference between the anodic and cathodic peaks cannot be precisely determined. The difference in oxidation/reduction peaks is somewhat higher than the theoretical value of ΔE_{pa-pc} = 59 mV, but both oxidation processes are essentially single-electron steps (resulting in radical cation and dication species, respectively). Recently, Bard et al. showed that 9,9-disubstituted terfluorenes show two consecutive reversible single-electron oxidation peaks with a difference $E_{2ox} - E_{1ox} \approx 0.16-0.17$ eV, which is close to our data (Table 2).[23] Thus, for longer oligomers due to delocalization of the charges along the arms, no substantial electronic interactions between the arms are observed and CV peaks belong to tris(radical cation) and tris(dication) species. For the shorter oligomer **T1**, the current value for the second oxidation is twice the height of the first one, and oligomer **T2** showed several overlapped oxidation peaks (Figure S1, Supporting Information). This could be a result of electronic interactions between the oligofluorene arms upon oxidation, which are not electronically isolated. Moreover, the central truxene core can also be involved in the oxidation process for short oligomers. All the oligomers are high-band-gap (E_g) materials; E_g^{CV} estimated from the difference between the onsets of the reduction wave and the first oxidation peak was found to vary in the range 3.20−3.40 eV (Table 2).

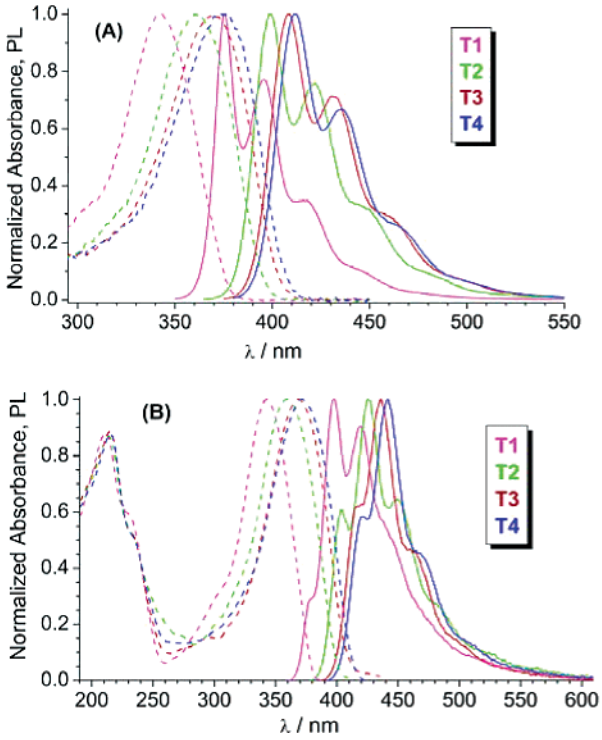

Figure 2. Absorption (dash lines) and photoluminescence (solid lines) spectra of truxene-oligofluorenes **T1**−**T4** in toluene (A) and in films (B).

(22) Geng, Y.; Trajkovska, A.; Katsis, D.; Ou, J. J.; Culligan, S. W.; Chen, S. H. *J. Am. Chem. Soc.* **2002**, *124*, 8337−8347.
(23) Choi, J.-P.; Wong, K.-T.; Chen, Y.-M.; Yu, J.-K.; Chou, P.-T.; Bard, A. J. *J. Phys. Chem. B* **2003**, *107*, 14407−14413.

Table 3. Optical Properties of Star-Shaped Oligofluorene-Truxene Derivatives **T1**−**T4**

compd	λ_{abs}, nm [log ϵ] (toluene)	λ_{abs}, nm (film)	λ_{PL}, nm (toluene)	λ_{PL}, nm (film)	Φ_{PL}[a] (toluene)	Φ_{PL}[a] (film)	E_g^{opt},[b] nm
T1	343 [4.97]	343	375sh, 396, 416sh	380sh, 398, 419.5	0.70	0.43	3.29
T2	360 [5.50]	359	399, 422, 443sh	404, 425.5, 449	0.83	0.51	3.14
T3	370 [5.61]	369	408, 431, 460sh	417sh, 436, 462sh	0.83	0.60	3.08
T4	374 [5.67]	372	411, 436, 460sh	422, 442, 467sh	0.86	0.59	3.05

[a] Estimated error in PL quantum efficiencies ~±10%. Quinine sulfate was used as a standard in estimation of PL efficiencies in solutions (Φ_{PL} = 0.546%). [b] Band gap estimated from the red edge of the longest wavelength absorption (in toluene).

Absorption and Emission Spectra. The absorption spectra for compounds **T1**−**T4** both in solution and in the solid state show strong $\pi-\pi^*$ electron absorption bands, which progressively red-shift with increasing chain length from 343 to 374 nm (Figure 2, Table 3). The maxima and shapes of the absorption peaks are the same for the solutions (cyclohexane or toluene) and films (Figure 2A, Figure S3, and Table 3), and the energies are in linear correlation (r = 0.998−0.999) with the inverse number of benzene units (n) in each arm (Figure S4). The absorption maxima corresponding to the energy values extrapolated to $n = \infty$ ($\lambda_{n=\infty}$ = 399 nm in cyclohexane or toluene, 396 nm in solid) are between the extrapolated values for linear oligofluorenes (402 nm in tetrahydrofuran) and the experimental value of λ_{max} = 388 nm for poly(9,9-dihexylfluorene).[6h] Oligomers **T1**−**T4** are highly fluorescent materials both in solution and in the solid state, with photoluminescence (PL) quantum efficiencies (Φ_{PL}) for higher oligomers close to those for linear polyfluorenes. PL spectra are red-shifted from **T1** to **T4** and show vibronic structure typical for polyfluorenes. An interesting feature of the solution-phase spectra is that the spectral shape is independent of conjugation length, as opposed to those for the solid state, where the vibrational progression bands change relative intensity. The band gaps for oligomers **T4**−**T1** of 3.05−3.29 eV, estimated from the red edge of the longest wavelength absorption in the electronic spectra, was found to be somewhat lower (by 0.11−0.16 eV) but still close to those determined from the electrochemical experiments (Tables 2 and 3).

Spectroscopy of Radical Cations. Considering the reversibility in the oxidation of oligomers **T1**−**T4** under CV conditions, we performed oxidative titration with 2,3-dichloro-5,6-dicyano-1,4-benzoquinone (DDQ)/CF_3CO_2H in DCM.[24] The radical cations generated show intense absorption in the visible region of the spectrum (497−572 nm) with red shifts from **T1** to **T4** (Figure 3).

Radical cations from truxene-oligofluorenes **T1**−**T4** have also been generated and studied by spectroelectrochemistry (SEC) (Figure 4; Figures S5−S7, Supporting Information). On electrochemical oxidation of compounds **T1**−**T4**, the intensity of absorption at ~340−400 nm decreased and new intense bands at ~460−600 nm appeared, the maxima and the shape of which corresponded well to the chemically generated radical cations (Figure 3). It should be noted that, on full conversion of the neutral molecules to radical cations, the short-wavelength bands (~340−400 nm) did not completely disappear (Figures 4A, S5, S6, and S7A). Upon further oxidation of the longer oligomers **T3** and **T4**, we also observed a decrease in the absorption maximum for the radical cation species and a hypsochromic shift of short-wavelength bands at more positive potentials

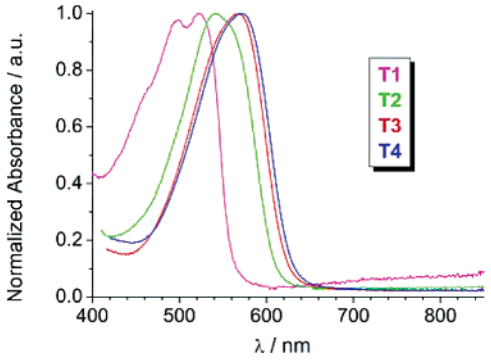

Figure 3. Absorption spectra of chemically generated radical cations from truxene-oligofluorenes **T1**−**T4** (λ_{max} = 497/525, 543, 567, and 572 nm, respectively).

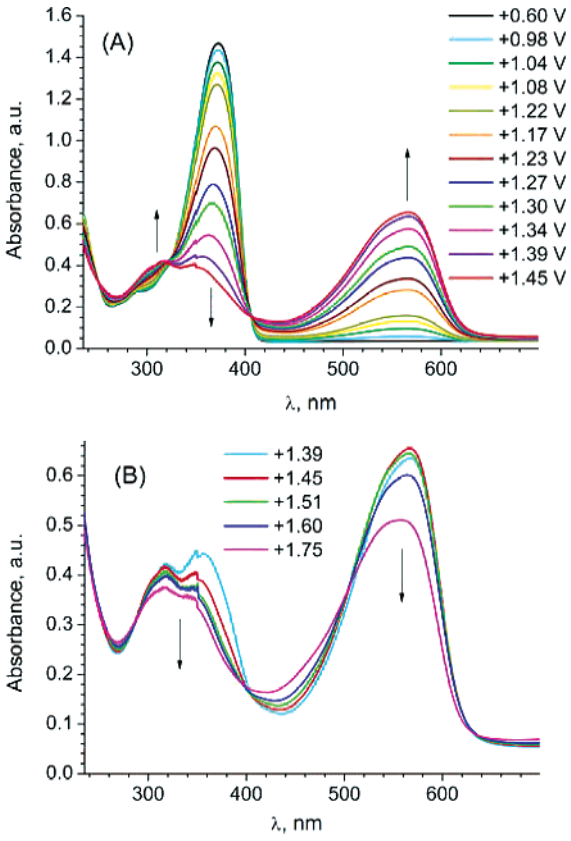

Figure 4. Spectroelectrochemistry of truxene-fluorene derivative **T3**, DCM, 0.1 M Bu_4NPF_6, Pt wire reference electrode. (A) Generation of radical cation from **T3**; (B) its further oxidation.

(Figures 4B and S7B). When the oxidation is limited to a potential range corresponding to the generation of radical cations, the process is completely reversible, and the initial spectra of the neutral species are completely restored. Several cycles of oxidation−reduction did not show any degradation of the

(24) Sep, W. J.; Verhoeven, J. W.; De Boer, Th. J. *Tetrahedron* **1979**, *35*, 2161−2168.

Table 4. Glass Transition Temperatures and Thermal Stability of Derivatives **T1**−**T4**

compd	M_w, g mol^{-1}	T_g,[a] °C	T_d,[b] °C [TGA, 5% mass loss]
T1	1844.95	63	401
T2	2842.52	86	408
T3	3840.08	101	410
T4	4837.65	116	413

[a] Measured at 10 °C/min. [b] Measured at 5 °C/min. When heating rate was increased to 25 °C/min, the decomposition temperatures were ca. 10−15 °C higher.

materials, providing further evidence for a highly reversible process. Thus, oligomers **T1**−**T4** reperesent reversible electrochromic systems with intense purple color in the oxidized state.

Thermogravimetric Analysis and Differential Scanning Calorimetry. For optoelectronic applications, the thermal and morphological stabilities are critical factors for device stability and lifetime. The compounds **T1**−**T4** demonstrated good thermal stability with no decomposition below 400 °C in an inert atmosphere (Table 4, Figure S8). The thermal stability of the oligomers was slightly increased from **T1** to **T4** by 10−15 °C. TGA experiments showed loss of ca. 45−50% of mass in the range of 420−480 °C for all the oligomers and further mass stability until 600 °C. This corresponds well to the abstraction of all hexyl substituents from the oligomers and probably results in stable polyarene materials. All of the oligomers are amorphous materials (some crystallinity is seen for **T1**) at room temperature, and their glass transition temperatures are improved from 63 °C for **T1** to 116 °C for **T4**. These values are 20−28 °C higher than those for the corresponding star-shaped oligofluorenes with a benzene central core,[15] while for the largest oligomer **T4** the glass transition temperature is even higher than that for poly(9,9-dihexylfluorene) (T_g = 103 °C; T_d = 390 °C).[25] Both linear and spiro-configured oligo(9,9-dialkylfluorenes) have been shown to possess comparable glass transition temperatures (∼60−150 °C), which vary substantially with the alkyl substituents at position 9 of the fluorene moiety.[6d,f,26] Heating films of the materials under a microscope using a cross-polarized configuration did not show any liquid crystalline behavior, contrary to what is generally observed in polyfluorenes.[27,4d] Furthermore, upon cooling, the materials stay in an amorphous glassy phase. The shapes of the fluorescence spectra and Φ_{PL} of the pristine spin-coated (from toluene) and thermally treated (150−200 °C, 0.5 h) films are essentially the same (within the error of the measurement), thereby confirming their good thermal and morphological stability.

Conclusion

In summary, we have presented a facile approach to highly luminescent soluble monodisperse star-shaped oligofluorenes with a truxene central core. The materials possess high thermal (>400 °C according to TGA) and electrochemical stability (to both p- and n-doping) and emit bright blue light ($\lambda_{PL} \approx$ 400−420 nm) with quantum efficiencies of ∼50−60% in the solid state. The two-dimensional architecture of these oligomers facilitates their increased stability toward self-association through arene−arene stacking, which improves the amorphous properties of the materials in the solid state. Excellent film-forming properties of the high-generation oligomers and nanoscale size of the macromolecules (∼1.7 × 7 nm for **T4**) make them potentially fascinating nano-objects for several optoelectronic applications, which are now under investigation. We also demonstrated electrochromic behavior of truxene-oligofluorenes **T1**−**T4**, which reversibly change their color from colorless in the neutral state (∼340−400 nm) to red or purple color in the oxidized state (∼500−600 nm).

Acknowledgment. We thank The Royal Society and NATO for a Postdoctoral Fellowship (A.L.K.) and NATO for an Expert Visit to Manchester (I.F.P.).

Supporting Information Available: Experimental Section (instrumentation, synthetic procedures, and characterization for all novel compounds, CV and spectroelectrochemistry experiments); CV, UV−vis, SEC, TGA, and molecular modeling details (Figures S1−S9; Table S1) (PDF). This material is available free of charge via the Internet at http://pubs.acs.org.

JA039228N

(25) Liu, B.; Yu, W.-L.; Lai, Y.-H.; Huang, W. *Chem. Mater.* **2001**, *13*, 1984−1991.
(26) Katsis, D.; Geng, Y. H.; Ou, J. J.; Culligan, S. W.; Trajkovska, A.; Chen, S. H.; Rothberg, L. J. *Chem. Mater.* **2002**, *14*, 1332−1339.
(27) (a) Grell, M.; Bradley, D. D. C.; Inbasekaran, M.; Woo, E. P. *Adv. Mater.* **1997**, *9*, 798−802. (b) Grell, M.; Redecker, M.; Whitehead, K.; Bradley, D. D. C.; Inbasekaran, M.; Woo, E. P. *Liq. Cryst.* **1999**, *26*, 1403−1407. (c) Sirringhaus, H.; Wilson, R. J.; Friend, R. H.; Inbasekaran, M.; Woo, E. P.; Grell M.; Bradley, D. D. C. *Appl. Phys. Lett.* **2000**, *77* 406−408.